Carcinogenesis vol.35 no.2 pp.396–406, 2014
doi:10.1093/carcin/bgt313
Advance Access publication September 26, 2013

Regulation of polarized morphogenesis by protein kinase C iota in oncogenic epithelial spheroids

Mark Linch[1,2], Marta Sanz-Garcia[1], Carine Rosse[1], Philippe Riou[1], Nick Peel[1], Chris D.Madsen[3], Erik Sahai[3], Julian Downward[4], Asim Khwaja[5], Christian Dillon[6], Jon Roffey[6], Angus J.M.Cameron[1] and Peter J.Parker[1,7,*]

[1]Department of Protein Phosphorylation, Cancer Research UK London Research Institute, London WC2A 3LY, UK, [2]Sarcoma Unit, Royal Marsden Hospital, London SW3 6JJ, UK, [3]Department of Tumour Cell Biology and [4]Department of Signal Transduction Laboratories, Cancer Research UK London Research Institute, London WC2A 3LY, UK, [5]Department of Haematology, UCL Cancer Institute, University College London, London WC1E 6BT, UK, [6]Cancer Research Technology Discovery Laboratories, Wolfson Institute for Biomedical Research, University College London, London WC1E 6BT, UK and [7]Division of Cancer Studies, King's College London, London SE1 1UL, UK

*To whom correspondence should be addressed. Tel: +44 (0) 207 269 3259; Fax: +44 (0) 207 269 3258;
Email: peter.parker@cancer.org.uk

Protein kinase C iota (PKCι), a serine/threonine kinase required for cell polarity, proliferation and migration, is commonly up- or downregulated in cancer. PKCι is a human oncogene but whether this is related to its role in cell polarity and what repertoire of oncogenes acts in concert with PKCι is not known. We developed a panel of candidate oncogene expressing Madin–Darby canine kidney (MDCK) cells and demonstrated that H-Ras, ErbB2 and phosphatidylinositol 3-kinase transformation led to non-polar spheroid morphogenesis (dysplasia), whereas MDCK spheroids expressing c-Raf or v-Src were largely polarized. We show that small interfering RNA (siRNA)-targeting PKCι decreased the size of all spheroids tested and partially reversed the aberrant polarity phenotype in H-Ras and ErbB2 spheroids only. This indicates distinct requirements for PKCι and moreover that different thresholds of PKCι activity are required for these phenotypes. By manipulating PKCι function using mutant constructs, siRNA depletion or chemical inhibition, we have demonstrated that PKCι is required for polarization of parental MDCK epithelial cysts in a 3D matrix and that there is a threshold of PKCι activity above and below which, disorganized epithelial morphogenesis results. Furthermore, treatment with a novel PKCι inhibitor, CRT0066854, was able to restore polarized morphogenesis in the dysplastic H-Ras spheroids. These results show that tightly regulated PKCι is required for normal-polarized morphogenesis in mammalian cells and that H-Ras and ErbB2 cooperate with PKCι for loss of polarization and dysplasia. The identification of a PKCι inhibitor that can restore polarized morphogenesis has implications for the treatment of Ras and ErbB2 driven malignancies.

Introduction

Protein kinase C iota (PKCι) is a serine/threonine kinase and an atypical member of the PKC family (aPKC), which is overexpressed and correlated with prognosis in a number of human malignancies (1–9). Several groups have reported anticancer effects of aPKC inhibitors although the mechanisms for this have not been fully elucidated (10–12). aPKC plays an important role in promoting apicobasal polarity of cells, mitotic spindle orientation, directional cell migration and epithelial barrier function; these functions are conserved from model organisms (*Caenorhabditis elegans* and *Drosophila melanogaster*) to humans (13–17).

The 'atypical' nomenclature of aPKC refers to the divergent regulatory domain compared with classical and novel PKCs in that it lacks a C2 domain and has an altered, DAG-insensitive C1 domain. Instead, aPKC has an N-terminal PB1 domain that interacts with the Par6-cdc42-GTP complex and probably, like other PKCs, the upstream regulatory domain interactors lead to allosteric activation by release of an inhibitory intramolecular interaction between the regulatory domain and the substrate-binding site (18,19). Activity also requires priming phosphorylations of the activation loop (T403/410) and turn motif (T555/556) by the upstream kinases, PDK1 (20) and likely TORC2, respectively (21,22). By analogy to other PKCs, nucleotide pocket occupation is likely to be important for determining the upstream kinase/phosphatase balance (23,24). However, beyond this the acute inputs that lead to activation of aPKC are poorly defined.

Cell polarity refers to the restriction of cellular components to particular regions of the cell (25,26). In epithelial monolayers, tight junctions form the boundary between the apical membrane surface and the basal membrane domain and with additional junctional complexes (adherens junctions) comprise the cell–cell contacts (27–29). Maintenance of these cell–cell contacts contributes to the survival of cells (release of normal epithelial cells from the monolayer causes anoikis) (30), to a restraint on proliferation through contact inhibition and to appropriate apical/basolateral receptor distribution and hence receptor-driven responsiveness (31,32).

Deregulation of polarity proteins is often associated with a more invasive phenotype in tumour model systems (33,34), and loss of apical–basal polarity in human epithelial cells is one of the hallmarks of aggressive and invasive cancers (35–37). Results from genetic screens in *D.melanogaster* suggest that aberrant expression of certain polarity genes (scrib, lgl and Crb) can lead to hyperplastic tumour formation in a wild-type (WT) background, whereas in an oncogenic Ras or Notch background they lead to invasive and metastatic tumours (38–41). Transgenic mouse studies have recently shown that deletion of the genes for Par4/LKB1 or Par3, two well-recognized polarity proteins, can contribute to tumour formation (32,42,43).

A number of studies have demonstrated physical and/or functional interactions between aPKC and *bona fide* human oncogenes such as phosphatidylinositol 3-kinase (PI3K) (44,45), Ras (46–49), Raf (50), ErbB2 (51) and Src (52,53). Equally, aPKC has been implicated genetically and through its *ex vivo* manipulation in the establishment and maintenance of polarity (54–56). However, it is quite unclear what the relationship is between the opposing aPKC functions of polarization and proliferation.

Madin–Darby canine kidney (MDCK) cells embedded in collagen matrix gels have been shown to form cysts that broadly recapitulate the morphological features of the renal collecting ducts from which they derive (57–59). As the cyst forms, there is central apoptosis, lumen formation (lumenogenesis) and localization of distinct proteins at the apical (facing lumen) or basal (facing outwards) plasma membranes. Suppression of aPKC, by RNA interference or dominant-negative constructs, has been shown to induce misorientation of the mitotic spindle, mispositioning of the nascent apical surface and ultimately the formation of aberrant cysts with multiple lumens (60–62).

Here, we have tested the relationship between the requirement for PKCι in the polarized morphology of MDCK cells and its role

Abbreviations: aPKC, atypical protein kinase C; cDNA, complementary DNA; GFP, green fluorescent protein; MDCK, Madin–Darby canine kidney; PBS, phosphate-buffered saline; PI3K, phosphatidylinositol 3-kinase; PKCι, protein kinase C iota; PSAL, predominant single apical lumen; siRNA, small interfering RNA; WT, wild-type.

in response to well-recognized human oncogenes that lead to altered epithelial morphology (51,63). Exploiting the MDCK cell model, we find that PKCι is required for the abnormal morphology caused by activated H-Ras and ErbB2, but not activated PI3K. This requirement appears to be a consequence of overactive PKCι since titration of PKCι function by small interfering RNA (siRNA) or with an aPKC-selective catalytic inhibitor partially corrects the abnormal H-Ras-induced morphology. All transformed derivatives displayed reduced proliferation on PKCι knockdown. Notably, PKCι displays a threshold behaviour with too little or too much activity causing loss of polarized organisation (dysplasia). These results implicate PKCι as a good therapeutic target in a subset of malignancies.

Materials and methods

Reagents

Reagents were purchased from Sigma unless otherwise specified. Mouse monoclonal PKCλ (610208), β-catenin (610154), GM130 (610823) and c-Raf (610151) antibodies were obtained from BD Biosciences. Rabbit monoclonal Her2 (2165) and rabbit polyclonal pPKCζ/λ (T410/403) (9378), pSrc (Y416) (2101), pSrc (Y527) (2105) antibodies were obtained from Cell Signaling. Rabbit polyclonal ZO-1 (40–2200) and pPKCι (T555) (44-968G) antibodies were obtained from Invitrogen. Alexa-555 goat anti-rabbit (A21429), Alexa-555 goat anti-mouse (A21422), Alexa-488 goat anti-mouse (A11001), Alexa-488 goat anti-rabbit (A11008) and Alexa-680 goat anti-rabbit (A21109) secondary antibodies were from Invitrogen. IR dye 800 goat anti-mouse (926-3221G) secondary antibody was from LI-COR Biosciences. IgG F(ab′)2 Goat anti-mouse blocking antibody (115-007-003) was from Jackson ImmunoResearch Labs. Go6983 was from Calbiochem and CRT0066854 was a gift from Cancer Research Technology.

Plasmids

Human PKCι complementary DNA (cDNA) (gifted from T.Biden) was subcloned into pEGFP-C1 vector (Clontech) incorporating a 5′-Myc-tag sequence and using 5′-SalI and 3′-BamHI restriction sites. The Entrez Nucleotide accession number is NM_002740.5. The cDNA contains two start codons at bp1-3 and bp28-30 with the second methionine denoted as the first amino acid of the protein. Green fluorescent protein (GFP)-PKCι mutants were generated using the QuikChange system (Stratagene). ErbB2-YVMA in a pEGFP-N1(A206K) vector was a gift from Tony Ng (Kings College London, UK).

siRNA and transfection

Transient reverse transfections of cDNA for MDCK cells were performed on Poly-L-lysine precoated plates using Lipofectamine 2000 as per the manufacturer's instructions (Invitrogen). siRNA reverse transfections of MDCK were performed using Lullaby (Oz Biosciences) and Poly-L-Lysine precoated plates. For a 6-well plate, 25 nM siRNA and 10μl Lullaby were mixed together in Optimen, incubated for 20 mins and added to 2–3 × 10^5 cells per well. Media was refreshed at 20 h and typically further manipulation took place 72 h posttransfection. Rescue experiments were performed by sequential transfection, initially using siRNA, as above, and then after 24 h cells were transfected using Lipofectamine 2000 and the appropriate cDNA. Knockdown efficiency was analysed by western blot and immunostaining of PKCι compared with the α-tubulin loading control. Target sequences for canine PKCι were 5′-AGTTCTGTTGGTGCGATTA-3′ (cfPKCι.1) and 5′-AAGCTCTGATAACCCGGATCA-3′ (cfPKCι.2) and scrambled controls were 5′-AATGAGTGAGTAGTCTTTGCT-3′ (cfSCRAM.1) and 5′-AAGGCCCAACGAAACCATACA-3′ (cfSCRAM.2).

Cell culture and stable cell lines

MDCK cells were obtained from Cell Production, Cancer Research UK. Isoenzyme and single nucleotide polymorphism analysis was performed by cell services to authenticate the origin of these cells. Cells were maintained in Dulbecco's modified Eagle's medium supplemented with 10% foetal bovine serum and PenStrep at 37°C in a humidified 5% CO_2 atmosphere. Stable MDCK cell lines expressing V12-Ras, p110-CAAX, v-Src or Raf-CAAX have been described previously (63). Stable ErbB2-MDCK cells were generated by liposomal transfection followed by selection with 750 g/ml G418 (GIBCO). These polyclonal cell lines were further selected based on moderate to high GFP expression by two successive rounds of fluorescence-activated cell sorting (CRUK FACS facility).

Three-dimensional lumenogenesis assay

The 3D culture of MDCK cells in Matrigel was performed as described previously (57,59,64). In brief, cells in log phase growth were trypsinized and resuspended in standard media supplemented with 2% low growth factor Matrigel (BD) at 2 × 10^4 cells/ml. Each well of an 8-well chamber slide (BD) was precoated with 30 μl of 100% Matrigel to which 400 μl of the cell suspension was added. Media-2% Matrigel was changed on alternate days for 5 days.

Immunofluoresence microscopy

MDCK cysts/spheroids grown in Matrigel on chamber slides were fixed with 2% formaldehyde in phosphate-buffered saline (PBS), washed in PBS and then permeabilized with 0.5% Triton X-100 in PBS. Alternatively, cysts/spheroids were released from Matrigel using ice-cold ethylenediaminetetraacetic acid–PBS, attached to poly-L-lysine-coated slides by centrifugation and then fixed and permeabilized as for the chamber slides. Immunostaining was carried out as described previously (65). After a quick rinse with PBS, cultures were mounted with Prolong Gold hard set mounting medium (Invitrogen).

MDCK cysts that had their F-actin stained with phalloidin were visualized with a confocal microscope (Zeiss 510) and an apical lumen assessment made. The middle of a cyst in the z plane was identified and the following criteria applied to determine whether the cyst has a 'predominant single apical lumen' (PSAL): (i) there must have been a clear continuous F-actin-defined lumen; (ii) the luminal actin staining must have been more intense than the basal (outside) staining; (iii) the unidimensional measurement of this lumen must have been at least one-third of the cyst diameter and (iv) the unidimensional measurement of the lumen must have been at least twice the size of any other luminal structure.

Western blotting

For immunoblotting, lysates or immunoprecipitates were resolved by sodium dodecyl sulphate–polyacrylamide gel electrophoresis and transferred to polyvinylidene difluoride membranes. Immunoblots were blocked in 3% bovine serum albumin–Tris-buffered saline containing 0.1% Tween 20 and probed with primary antibodies as indicated. Following incubation with appropriate secondary antibodies, bands were visualized using the Odyssey infrared imaging system (LI-COR Biosciences). The quantification of the bands was performed using the Gel function on ImageJ version 1.40g.

Statistical analysis

Differences between the treatment groups were assessed by analysis of variance with a repeated measurement module using statistical software (GraphPad Prism; version 5.0d). P values of <0.05 were regarded as significant.

Results

Loss of polarity in Ras- and ErbB2-transformed MDCK cells requires PKCι

To assess the apparently anomalous requirement for PKCι in normal-polarized cells and oncogene-dependent depolarized growth, we established an MDCK cell 3D culture model and various oncogene-driven variants. This cell model lends itself to functional analysis of PKCι and circumvents the possible redundant function of PKCζ, the closely homologous aPKC, as there is comparatively little PKCζ protein in MDCK cells (56). Furthermore, cysts can form within 6 days of culture in Matrigel (Supplementary Figure S1A, available at *Carcinogenesis* Online), displaying typical polarized features (Supplementary Figure S1B, available at *Carcinogenesis* Online) and enabling siRNA-driven knockdown and transient expression studies to be undertaken within this time window.

Contrary to the polarized behaviour of the parental cell line, Raf-CAAX-, v-Src-, p110α-CAAX-, V12H-Ras- and ErbB2-transformed MDCK cell lines all grow in 3D culture with enlarged, aberrant or no overt polarization (Figure 1A). In particular, H-Ras-MDCK and p110α-MDCK grew as large, non-polarized spherical aggregates that lacked an apical (central) lumen and an apical actin ring. The v-Src cells developed with a large central lumen surrounded by multiple smaller lumens. The Raf-MDCK cells formed as large but otherwise apparently normal cysts. As many of these structures derived from the oncogenic MDCK cell lines were not cysts, we refer to them as oncogenic MDCK spheroids.

In 2D culture, parental cells grew as clusters and at confluence adopted a characteristic cobblestone appearance (57). As a monolayer, the MDCK variants that expressed H-Ras, p110α and v-Src were more fibroblastic in appearance and lost their direct cell–cell contacts, an appearance most pronounced in H-Ras-MDCK cells (Figure 1A).

Each oncogene expressing MDCK cell line was shown to overexpress their defining oncogenic protein by western blot analysis (Figure 1B). Similar protein loading was demonstrated with tubulin

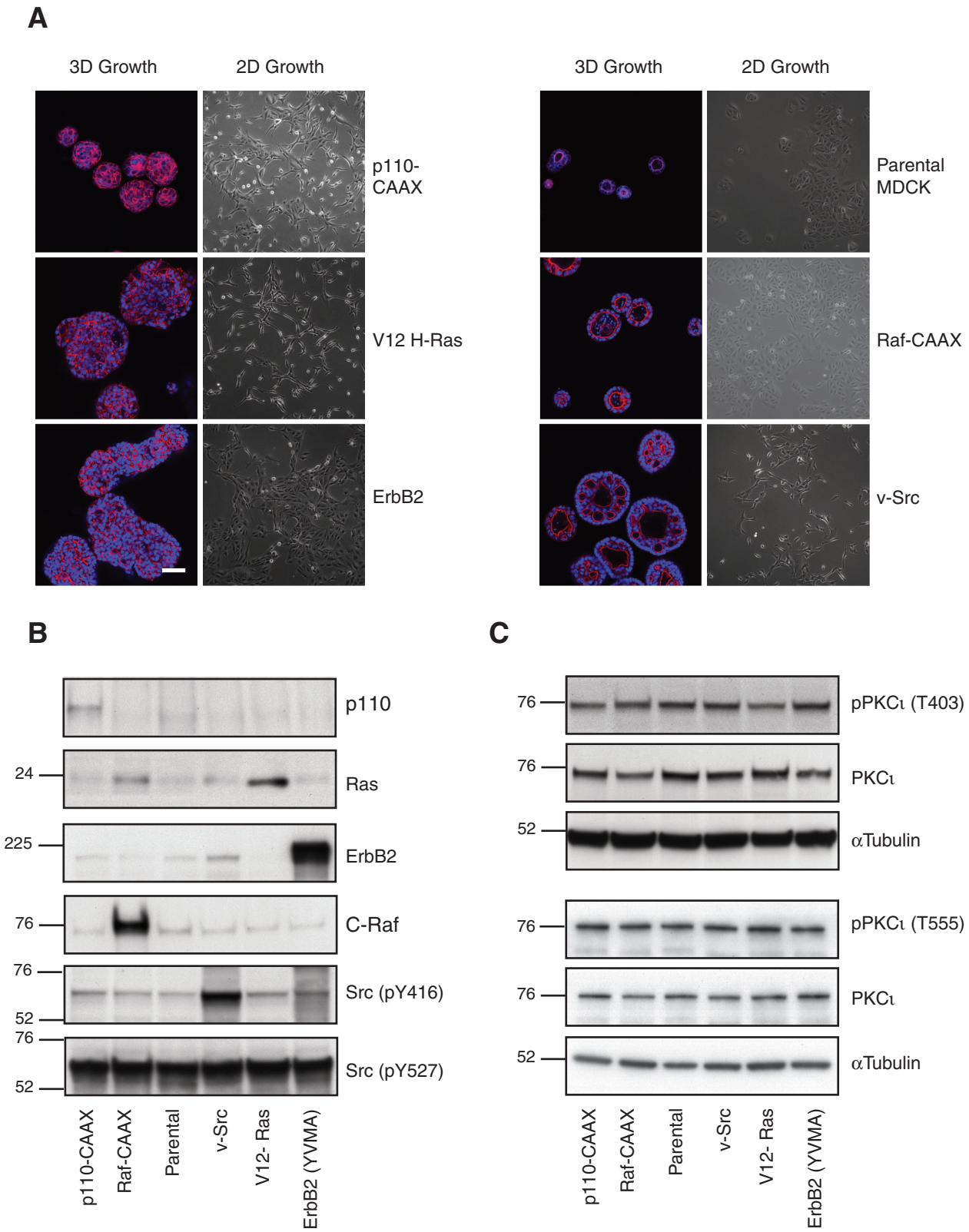

Fig. 1. Characterization of oncogenic MDCK cells. (**A**) MDCK cell variants cultured in Matrigel (3D) for 6 days alongside phase images of their growth in 2D. Phalloidin (red)-stained actin and Hoechst (blue)-identified nuclei. Scale bar represents 50 μm. Lysates of MDCK oncogenic variant cell lines in log phase growth were immunoblotted for (**B**) defining proteins and (**C**) phospho-PKCι/total PKCι.

or the consistent phosphorylation of c-Src at tyrosine 527, a residue that is present in normal cellular c-Src but deleted in constitutively active v-Src (66). Total PKCι levels were similar between the parental MDCK cells and the oncogenic MDCK cell panel. Phosphorylation of the activation loop of PKCι at threonine 403 or the turn motif at threonine 555 have been suggested as a possible markers of PKCι activity (67,68). However, phosphorylation at these sites were uniform for the parental and oncogenic MDCK cells (Figure 1C), (see Discussion).

To further examine whether cooperation between the activated oncogenes and PKCι contributed to the loss of apical lumen formation and loss of polarity, PKCι was transiently downregulated in each of the oncogene expressing MDCK cell lines using two distinct canine PKCι-directed siRNA duplexes. From initial studies in ErbB2 spheroids, it was striking that siRNA-PKCι led to reconstitution of an apical lumen and apical actin staining although in most cases this did not lead to the appearance of a fully normal MDCK cyst. In order to capture these differences objectively, an alternative parameter was defined as PSAL (see Materials and methods). The reproducibility of this scoring was validated and applied to subsequent experiments.

In both H-Ras and ErbB2-MDCK spheroids, but not v-Src (Figure 2A and B), p110α or Raf (Supplementary Figure S2A and B, available at *Carcinogenesis* Online) expressing cells, knockdown of PKCι resulted in significantly more PSAL spheroids. In the p110α-transformed spheroids, there was no difference in PSAL score between the siRNA-PKCι and the scrambled control, but unlike the Raf-MDCK spheroids, apical lumens were rarely present at all and knockdown was efficient (Supplementary Figure S2, available at *Carcinogenesis* Online). Upon PKCι knockdown of the parental MDCK cells, <50% of spheroids contained a PSAL compared with over 70% in the group treated with the scrambled control siRNA (Figure 2A and B). The maximal PKCι knockdown efficiency by the siRNA duplexes was between 70 and 80% depending on cell line, except for Raf-expressing cells where the level of knockdown was consistently <40% (Figure 2C). It must be noted that assessment of PKCι abundance in 3D was hampered by a poor signal to noise when lysates were generated following cold ethylenediaminetetraacetic acid extraction from Matrigel and therefore the PKCι knockdown was monitored in the parallel 2D cultures 72 h post-transfection. However, we have subsequently demonstrated that siRNA-PKCι knockdown of parental 3D MDCK cysts closely mirrors the level of knockdown of 2D MDCK at 72 h posttransfection.

To determine the specificity of the siRNA utilized in these knockdown studies, we rescued the siRNA-induced phenotype with a siRNA-resistant cDNA of PKCι. Human PKCι-cDNA differed from the homologous region of the canine siPKCι.2 by four non-consecutive nucleotides and this proved to be resistant to the canine siRNA (Figure 3A and B). H-Ras-MDCK cells were transfected sequentially, first with siPKCι and then after 24 h with the human cDNA for PKCι. Following co-transfection of H-Ras-MDCK cells with siPKCι.2 and empty vector (Figure 3C), there was a >3-fold increase in the number of spheroids displaying PSAL compared with the scrambled control (Figure 3D). When the Ras-MDCK cells were treated with siPKCι.2 and transfected with the resistant PKCι-cDNA the increase in spheroids with PSAL was attenuated (<2-fold). Note that the biphasic/threshold behaviour of the system is such that obtaining a precise, quantitative rescue is very difficult to achieve. Addition of PKCι to the scrambled control siRNA had little effect on the number of PSALs. Thus, a partial rescue of the siRNA-PKCι-induced phenotype with cDNA-PKCι was attained. These data are consistent with a model in which PKCι acts in cooperation with oncogenic Ras in determining transformed MDCK cell morphology.

PKCι depletion results in selective growth inhibition of oncogenic MDCK spheroids

In the multi-lumen, polarized morphology assay, the PKCι-depleted cysts were significantly smaller than control structures in keeping with previous reports that have demonstrated decreased growth as a consequence of increased apoptosis upon aPKC inhibition or depletion (60,68). To quantify this decreased growth, multiple phase images were taken of each oncogenic spheroid condition following 6 days growth in Matrigel (Figure 4A) and the mean cross-sectional area was calculated as an estimation of size (Figure 4B–G). All transformed MDCK cells lines treated with scrambled control siRNA (siSCRAM) showed larger spheroids than the parental MDCK. Surprisingly, although the effect of PKCι knockdown on the multi-lumen phenotype was limited to the H-Ras and ErbB2-MDCK spheroids (Figure 2A and B), all oncogenic spheroids were decreased in size with the exception of the parental cell line, which was insensitive to any growth inhibition (Figure 4B–G).

The implication of the preceding data is that PKCι cooperates with various oncogenes to support 3D growth and that for a subset of these (Ras, ErbB2), PKCι protein and/or activity contributes to the loss of polarity. Furthermore, the recovery of polarity on reduction of PKCι in Ras- and ErbB2-transformed MDCK cells suggested that an overactive PKCι was responsible for this aberrant behaviour. In contrast, in the parent cell, loss of PKCι has been reported to trigger loss of polarity suggesting that in fact the PKCι dependence displays threshold behaviour (60,61,69). To test this, we manipulated gain and loss of function of PKCι in the parental MDCK cells. A conformationally normal, inactive, siRNA-resistant PKCι mutant (PKCι-D368N) was employed to generate a stable cell line. In addition, stable MDCK cells lines with constitutively active PKCι (PKCι-A120E), PKCι-WT and empty vector (GFP) were generated to examine the role of a graded increase in PKCι activity in MDCK lumenogenesis. Comparable levels of exogenous and endogenous PKCι in the stable cells lines were confirmed by western blot (Supplementary Figure S3, available at *Carcinogenesis* Online). Following 6 days growth in Matrigel, normal lumenogenesis (~50% normal cysts) was seen for empty vector controls and for PKCι-WT, although for the latter there was a non-significant increase in cyst size (Figure 5A and B). Notably, an increase in abnormal, multi-lumen cyst phenotype was seen following depletion of PKCι with siRNA (Figure 5C and D) and also in the PKCι-D368N-expressing cells (Figure 5A and B). Unexpectedly, there was also an increase in multi-lumen formation on expression of the activated mutant PKCι-A120E-expressing cysts (Figure 5A and B).

This pattern of behaviour in response to manipulation of PKCι provides clear evidence for threshold behaviour—too little or too much triggering aberrant polarized morphology in 3D culture. The equivalent levels of expression of the different mutants suggest that this behaviour is dependent on catalytic activity and not protein *per se*, consistent with the marked effect of the constitutively active pseudosubstrate site mutant.

A novel PKCι inhibitor restores apical lumen formation

To assess this threshold, predicted catalytic behaviour of PKCι, we determined the response to the catalytic inhibitors CRT0066854, a recently described thieno[2,3-d]pyrimidine-based chemical inhibitor of aPKC (69), and Gö6983 (a pan PKC inhibitor) in H-Ras MDCK spheroids. Inhibitors were added on the day of seeding a single cell suspension in Matrigel and then replenished on alternate days for 6 days. The inhibitor doses used for compounds were determined based on their individual, previously defined cellular IC50s (69,70). Both inhibitors phenocopied the siRNA-PKCι intervention resulting in the induction of apical lumen formation in the spheroids and a reduction in spheroid size (Figure 6). The maximal effect of Gö6983 was at 2 μM resulting in a 6-fold increase in PSALs (Figure 6A and C). The maximal proportion of spheroids with PSALs was seen with CRT0066854 at the lower dose of 1.2 μM (Figure 6B and D). Above these doses, there was increasing cell death making scoring of apical lumens unreliable. The response to these inhibitors is entirely consistent with a requirement for oncogene-induced, elevated activity of PKCι to retain non-polarized proliferation.

Discussion

We have assessed the relationship between PKCι action in establishing polarity in the 3D MDCK cyst cell model, with its role in the growth and aberrant morphology associated with oncogene transformation. Under normal conditions, it was confirmed that loss of PKCι function was associated with a loss of polarized MDCK cyst formation. However, it was also demonstrated that constitutive activation of PKCι also caused a loss of polarity. Evidently, there is a window in which a normal level of regulated PKCι needs to function to support polarization. The loss of polarity consequent to transformation by Ras and ErbB2, but not selected isoforms of PI3K, Raf or Src, was associated with a gain of PKCι activity, since knockdown or inhibition of catalytic activity could partially restore a polarized morphology. This

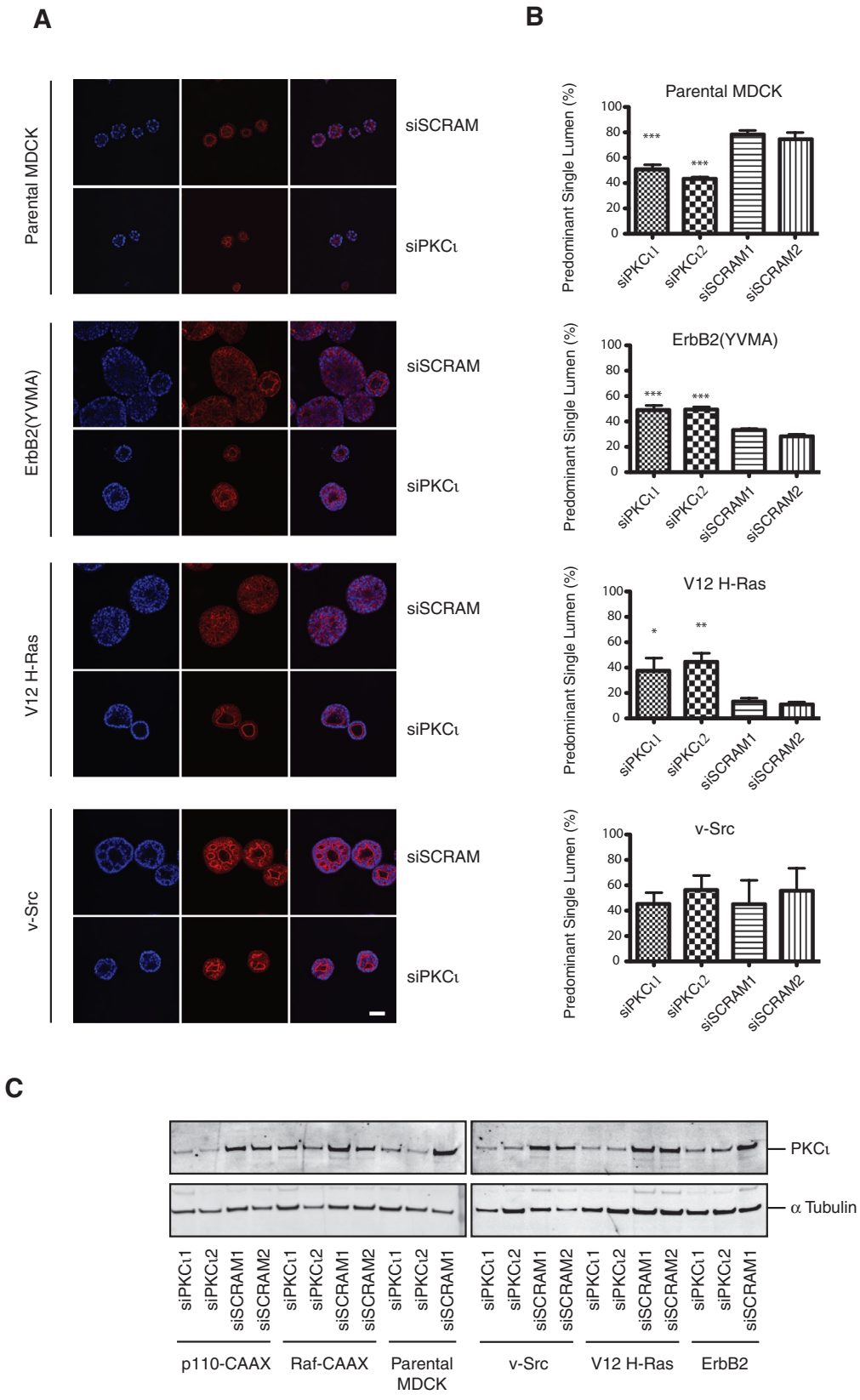

Fig. 2. The effect of PKCι knockdown on polarized morphogenesis of oncogenic MDCK spheroids. MDCK oncogenic variant cell lines were treated with two separate siRNA-PKCι (siPKCι1 and siPKCι2) and two scrambled controls (siSCRAM1 and siSCRAM2) for 24 h prior to culture in Matrigel for 6 days. (**A**) Representative single confocal images with phalloidin (red)-stained actin and Hoechst (blue)-identified nuclei. Scale bar represents 50 μm. (**B**) Quantification of number of PSALs. At least 100 spheroids were counted per condition and the mean and standard error of the mean of at least three separate experiments are presented. The statistical differences between PKCι knockdown conditions and the corresponding scrambled controls are shown; $*P < 0.05$; $**P < 0.01$; $***P < 0.001$. (**C**) PKCι protein depletion was confirmed in adherent cells 2 days after reseed (72 h after transfection) by western blot.

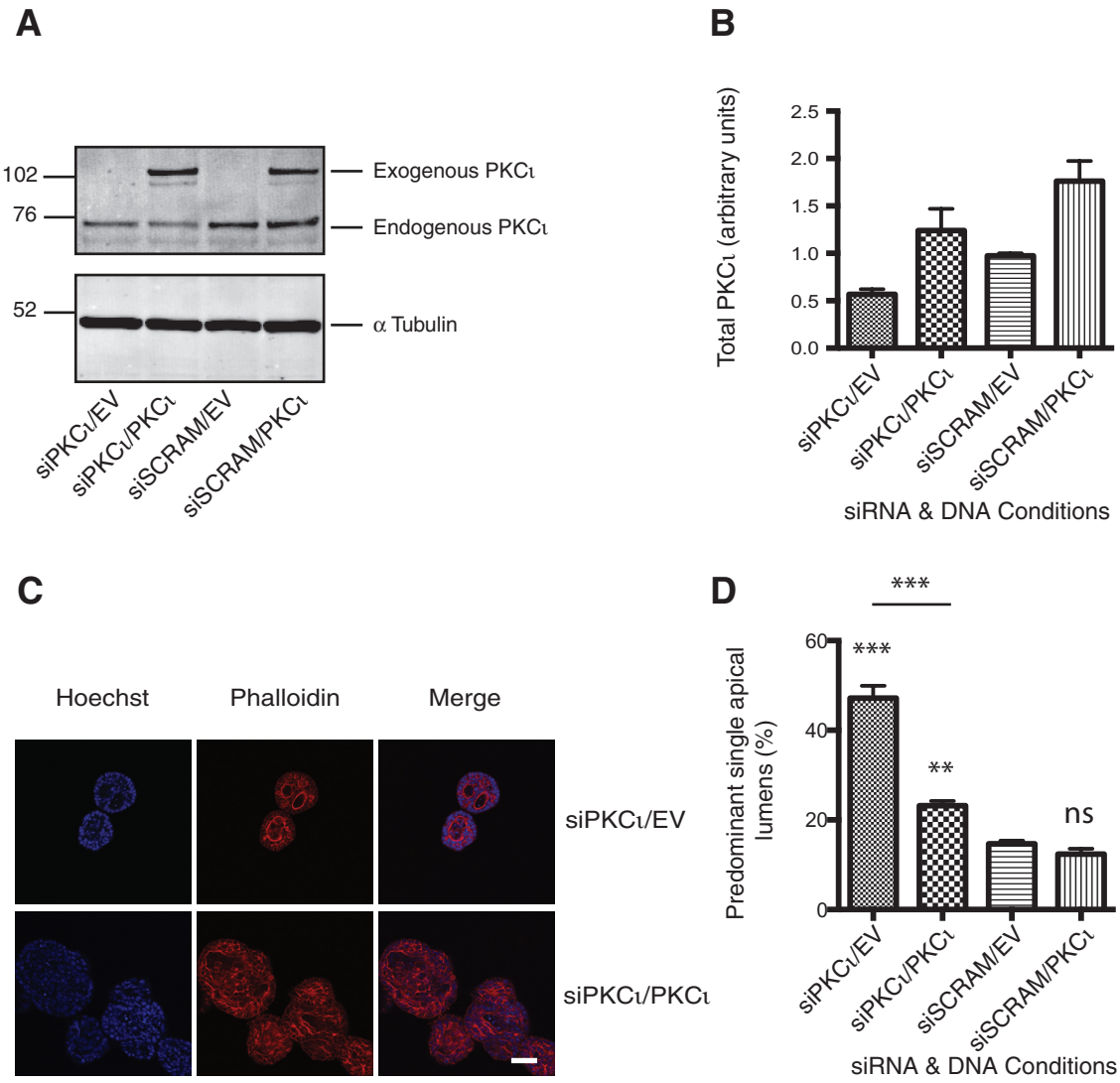

Fig. 3. Rescue of siRNA-induced polarity phenotype by cDNA-PKCι. H-Ras-MDCK cells were sequentially transfected with siRNA-PKCι or scrambled control (siSCRAM) followed by siRNA-resistant PKCι-cDNA or empty vector (EV). Cells were reseeded in 6-well plates (**A** and **B**) or Matrigel (**C** and **D**) 24 h after second transfection. (**A**) The levels of endogenous PKCι knockdown and GFP-PKCι overexpression were determined by western blot 24 h after reseed. (**B**) Densitometry was performed on the resulting blots using ImageJ software. (**C**) The sequentially transfected cells were seeded in Matrigel and cultured for 6 days. Representative single confocal images of phalloidin (red)-stained actin and Hoechst (blue)-identified nuclei are shown. Scale bar represents 50 μm. (**D**) Quantification of the number of predominant single lumens is shown. At least 100 spheroids were counted per condition and the mean and standard error of the mean for three separate experiments are presented. The statistical differences of treatments compared with siSCRAM/EV control are shown: ns, not significant; $^{**}P < 0.01$; $^{***}P < 0.001$.

indicates that Ras- and ErbB2-induced transformation upregulates the function of PKCι, pushing it beyond the threshold required to retain cyst polarity. In parental MDCK cysts, depletion of PKCι triggered loss of polarity. Although this may be a consequence of different PKCι-dependent signalling pathways in the different cell lines, in light of the data from the exogenous expression of PKCι activity mutants, this supports the role of required thresholds of PKCι abundance/activity. Given the multitude of effects of Ras and ErbB2 transformation on cell signalling, it is somewhat surprising that PKCι knockdown or chemical inhibition can acutely reverse (albeit partially) the abnormal non-polarized epithelial morphology but this is particularly interesting in the context of potential therapeutic interventions.

Despite the clear PKCι-dependent multi-lumen formation, we did not find altered regulation of total PKCι levels or PKCι phosphorylation at the activation loop (pT403) or turn motif (pT555). Several groups have reported pT403/pT555 PKCι as an activity readout (67,68,71); however, because PKCs are typically constitutively phosphorylated it is not entirely surprising that altered phosphorylation is not detected (72). It is surmised that other modifications or more fleeting allosteric inputs to PKCι are engaged in this depolarising pathway. In this context, it is notable that despite a number of proposed mechanisms for Ras to influence PKCι there is no consensus mechanism defined. Given the known aPKC-PI3K interplay (44,45,73), and that the pan-PI3K inhibitor, LY294002, has been reported to reverse the depolarized morphology of human mammary cell line spheroids (74), it was perhaps surprising that PKCι depletion/inhibition was unable to rescue the polarity of p110α-transformed spheroids. Given the evident sensitivity of PKCι to inhibition by the agents employed here, it can be surmised that the effects of p110α on morphology are triggered through one of the many other pathways dependent on phosphatidylinositol (3,4,5) trisphosphate. Reciprocally, the lack of connection between aPKCι and the PI3K pathway is indicative, in this context, of aPKCι control operating through its upstream regulators (PDK1, TORC2, cdc42; see Introduction) in a manner that is not rate-limiting for phosphatidylinositol (3,4,5) trisphosphate production and reflecting the finding that its direct interaction with anionic phospholipids is not unique to phosphatidylinositol (3,4,5) trisphosphate (75).

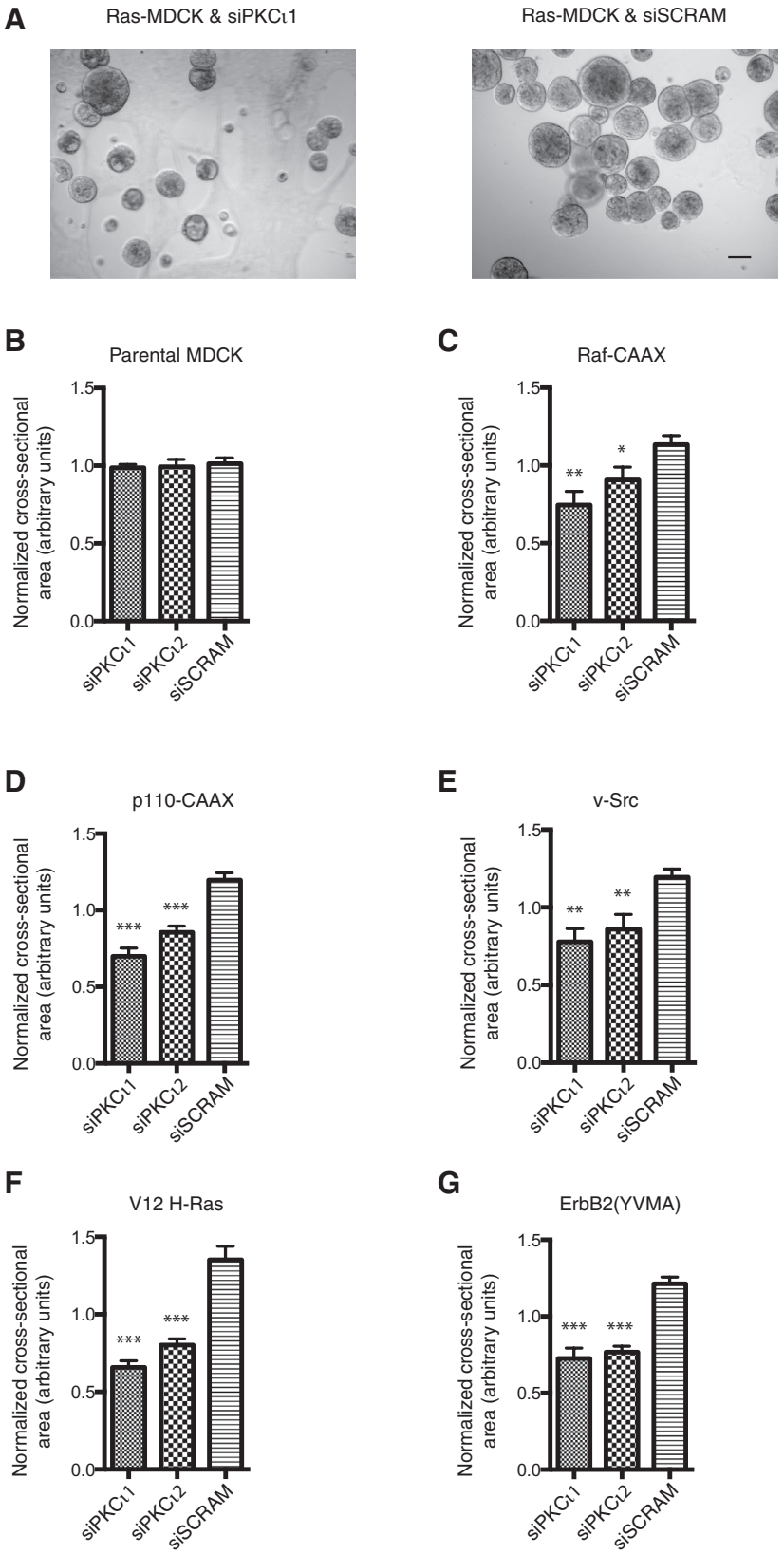

Fig. 4. The effect of PKCι knockdown on the size of oncogenic MDCK spheroids. MDCK oncogenic variant cell lines were treated with two separate siRNA-PKCι (siPKCι1 and siPKCι2) and scrambled control (siSCRAM) for 24 h prior to culture in Matrigel for 6 days. (**A**) Representative single phase images are shown. Scale bar represents 50 μm. (**B**–**G**) Quantification of the normalized cross-sectional area of the spheroid lumens. At least 100 spheroids were counted per condition and the mean and standard error of the mean of at least three separate experiments are presented. Statistical significance of differences between PKCι knockdown conditions and the scrambled control is shown: $*P < 0.05$; $**P < 0.01$; $***P < 0.001$.

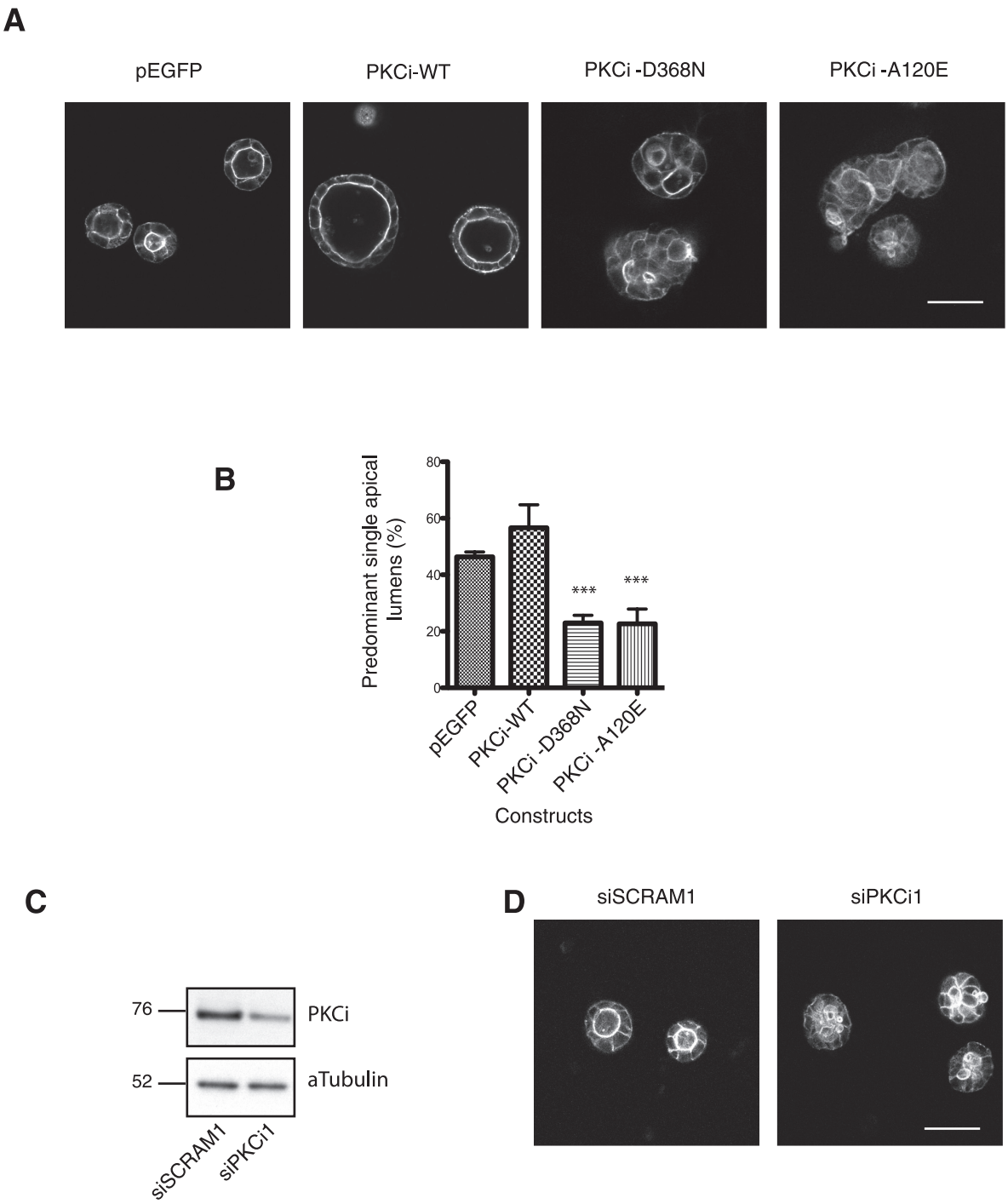

Fig. 5. Manipulation of PKCι impacts on apical lumen formation in MDCK cells. MDCK cells stably transfected with empty vector (pEGFP), PKCι-WT or activity mutants; kinase dead (PKCι-D368N) or constitutively active (PKCι-A120E) were cultured in Matrigel for 6 days. (**A**) Representative single confocal images of actin staining (white) are presented. (**B**) Quantification of the number of PSALs. At least 100 spheroids were counted per condition and the mean and standard error of the mean of three separate experiments are presented. Statistical significance of any differences compared with the WT-PKCι are shown: ***$P < 0.001$. (**C**) Representative western blot of three separate experiments showing the level of knockdown of endogenous PKCι by siRNA (siPKCι) or scrambled control (siSCRAM). (**D**) Representative single confocal images of actin staining (white) are presented. All scale bars represent 50 μm.

To our knowledge, oncogenic Ras has not previously been directly implicated as cooperating with aPKC in depolarized morphology in mammalian cells. The role in transformation; however, is more firmly established with both a Ras>PKCι>Rac1 axis (47,76) and synergism between Ras and PKCι for colony formation of ovarian cancer cells described (77). Furthermore, mice bitransgenic for oncogenic K-Ras and Cre-dependent loss of PKCι developed fewer lung tumours upon Cre-delivery (78). The cooperation between PKCι and ErbB2 seen in our study is consistent with the report in the MCF10a acini model, whereby genetic disruption of Par6 binding to aPKC rescued ErbB2-induced loss of apical lumen formation and polarity (51). Intriguingly, the Oncomine dataset of human epithelial malignancies revealed that high levels of PKCι transcripts are concomitantly expressed with Ras and Her2 but not isoforms of PI3K, Raf or Src. This further suggests the target population for trials of PKCι inhibitors might usefully focus on Ras and/or ErbB2 mutant/upregulated tumours, a group that is

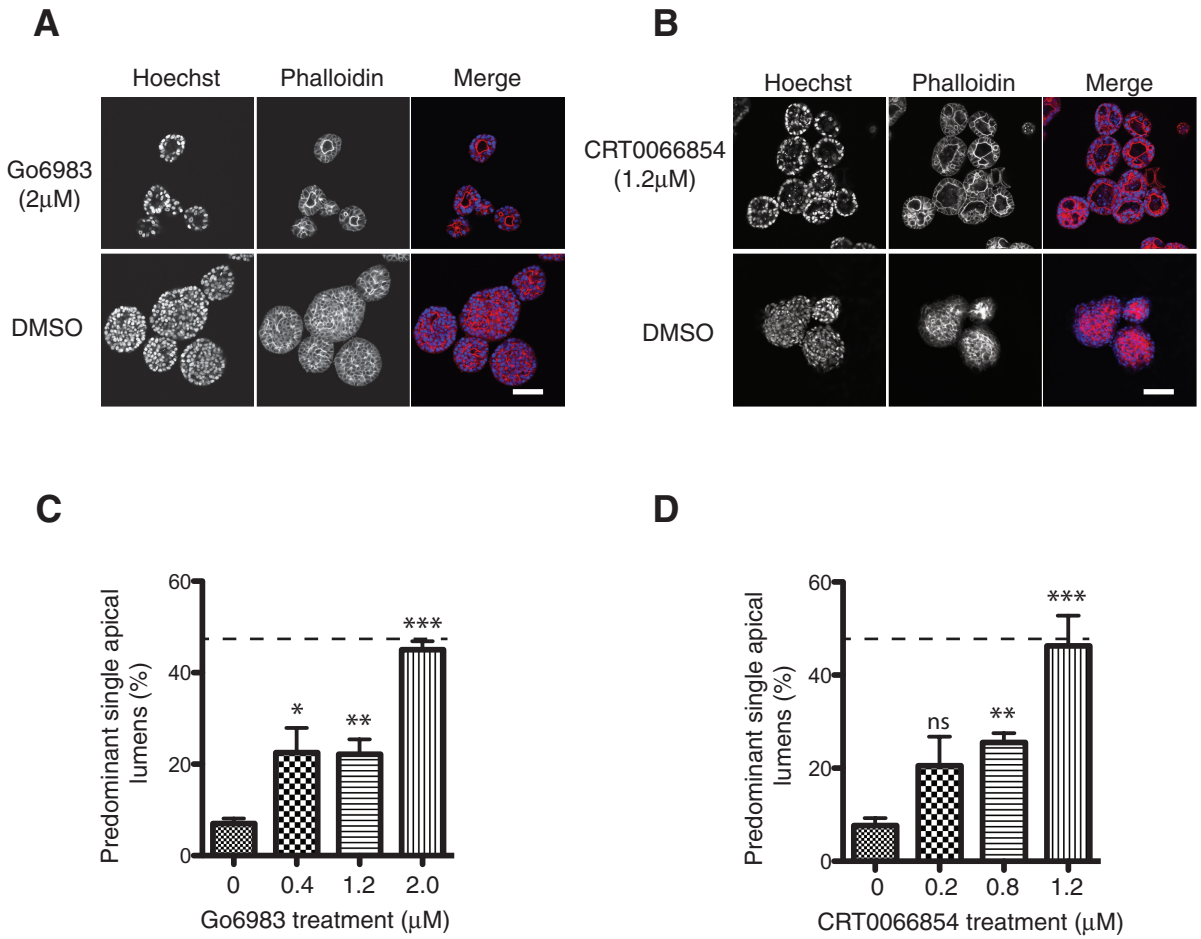

Fig. 6. PKCι inhibitors restore lumen formation in H-Ras-MDCK spheroids. H-Ras-MDCK cells were cultured in Matrigel for 6 days and treated with inhibitors at a range of concentrations. Representative single confocal images of H-Ras-MDCK spheroids treated with; (**A**) 2.0 μM Go6983 and (**B**) 1.2 μM CRT0066854 are presented. Spheroids were fixed and stained for actin (red) and DNA (blue). Scale bars represent 50 μm. (**C** and **D**) Quantification of the number of PSALs at different inhibitor concentrations. At least 100 spheroids were counted per condition and the mean and standard error of the mean are presented for at least three separate experiments. The dotted line represents the percentage PSALs seen in the parental MDCK cysts (see Figure 1). Statistical significance of differences between inhibitor-treated and dimethyl sulphoxide (DMSO) control is shown: ns, not significant; *$P < 0.05$; **$P < 0.01$; ***$P < 0.001$.

estimated to encompass at least 30% of human tumours (COSMIC: www.sanger.ac.uk/genetics/CGP/cosmic, Gene Expression Atlas: www.ebi.ac.uk/arrayexpress).

The loss of polarized morphogenesis upon PKCι inhibition or depletion in normal cells questions whether PKCι is a suitable drug target. It has been proposed that disruption of cellular polarity facilitates oncogenic proliferation by releasing epithelial cells from structural or signaling constraints by the basement membrane (31,32). However, although PKCι depletion led to decreased growth in all transformed MDCK cell variants, in normal MDCK cells we did not observe any change in 3D cyst size despite the disrupted polarized morphogenesis. Our results suggest that PKCι has both growth and polarity functions depending on the cooperative oncogenic context. Therefore, if proliferation is inhibited, disruption in polarity may not be expected to be an oncogenic event in normal cells establishing an anticipated therapeutic index for PKCι inhibitors.

In conclusion, PKCι loss or gain of function disrupts normal-polarized behaviour of MDCK cells, indicative of a threshold requirement for this kinase. In the context of cooperation with oncogenic Ras for the reversible depolarization of MDCK, this reflects hyperactivation (gain of function) of PKCι based on recovery following PKCι inhibition. This oncogene-dependent PKCι hyperactivation is pro-proliferative in 3D culture, providing compelling evidence that PKCι will be a good target for Ras mutant tumours.

Supplementary material

Supplementary Figures S1–S3 can be found at http://carcin.oxfordjournals.org/

Funding

Cancer Research UK; Royal Marsden/Institute of Cancer Research National Institute for Health Research Biomedical Research Centre (M.L.).

Acknowledgements

We would like to thank T.Ng for the ErbB2 construct and to Cancer Research Technology for supply of CRT0066854. We would like to thank J.Claus for help with graphics and to all members of the Parker Lab for critical reading.

Conflict of Interest Statement: None declared.

References

1. Eder,A.M. *et al.* (2005) Atypical PKCiota contributes to poor prognosis through loss of apical-basal polarity and cyclin E overexpression in ovarian cancer. *Proc. Natl Acad. Sci. USA*, **102**, 12519–12524.

2. Ishiguro,H. *et al.* (2009) aPKClambda/iota promotes growth of prostate cancer cells in an autocrine manner through transcriptional activation of interleukin-6. *Proc. Natl Acad. Sci. USA*, **106**, 16369–16374.
3. Kojima,Y. *et al.* (2008) The overexpression and altered localization of the atypical protein kinase C lambda/iota in breast cancer correlates with the pathologic type of these tumors. *Hum. Pathol.*, **39**, 824–831.
4. Li,Q. *et al.* (2008) Correlation of aPKC-iota and E-cadherin expression with invasion and prognosis of cholangiocarcinoma. *Hepatobiliary Pancreat. Dis. Int*, **7**, 70–75.
5. Patel,R. *et al.* (2008) Involvement of PKC-iota in glioma proliferation. *Cell Prolif.*, **41**, 122–135.
6. Regala,R.P. *et al.* (2005) Atypical protein kinase C iota is an oncogene in human non-small cell lung cancer. *Cancer Res.*, **65**, 8905–8911.
7. Scotti,M.L. *et al.* (2010) Protein kinase Ciota is required for pancreatic cancer cell transformed growth and tumorigenesis. *Cancer Res.*, **70**, 2064–2074.
8. Takagawa,R. *et al.* (2010) High expression of atypical protein kinase C lambda/iota in gastric cancer as a prognostic factor for recurrence. *Ann. Surg. Oncol.*, **17**, 81–88.
9. Wang,J.M. *et al.* (2009) Significance and expression of atypical protein kinase C-iota in human hepatocellular carcinoma. *J. Surg. Res.*, **154**, 143–149.
10. Erdogan,E. *et al.* (2006) Aurothiomalate inhibits transformed growth by targeting the PB1 domain of protein kinase Ciota. *J. Biol. Chem.*, **281**, 28450–28459.
11. Guo,W. *et al.* (2008) Identification of a small molecule with synthetic lethality for K-ras and protein kinase C iota. *Cancer Res.*, **68**, 7403–7408.
12. Pillai,P. *et al.* (2011) A novel PKC-ι inhibitor abrogates cell proliferation and induces apoptosis in neuroblastoma. *Int. J. Biochem. Cell Biol.*, **43**, 784–794.
13. Calcagno,S.R. *et al.* (2011) Protein kinase C iota in the intestinal epithelium protects against dextran sodium sulfate-induced colitis. *Inflamm. Bowel Dis.*, **17**, 1685–1697.
14. Iden,S. *et al.* (2012) aPKC phosphorylates JAM-A at Ser285 to promote cell contact maturation and tight junction formation. *J. Cell Biol.*, **196**, 623–639.
15. Izumi,Y. *et al.* (1998) An atypical PKC directly associates and colocalizes at the epithelial tight junction with ASIP, a mammalian homologue of Caenorhabditis elegans polarity protein PAR-3. *J. Cell Biol.*, **143**, 95–106.
16. Tabuse,Y. *et al.* (1998) Atypical protein kinase C cooperates with PAR-3 to establish embryonic polarity in Caenorhabditis elegans. *Development*, **125**, 3607–3614.
17. Wald,F.A. *et al.* (2011) Aberrant expression of the polarity complex atypical PKC and non-muscle myosin IIA in active and inactive inflammatory bowel disease. *Virchows Arch.*, **459**, 331–338.
18. Parker,P.J. *et al.* (2004) PKC at a glance. *J. Cell Sci.*, **117**(Pt 2), 131–132.
19. Yamanaka,T. *et al.* (2001) PAR-6 regulates aPKC activity in a novel way and mediates cell-cell contact-induced formation of the epithelial junctional complex. *Genes Cells*, **6**, 721–731.
20. Le Good,J.A. *et al.* (1998) Protein kinase C isotypes controlled by phosphoinositide 3-kinase through the protein kinase PDK1. *Science*, **281**, 2042–2045.
21. Guertin,D.A. *et al.* (2006) Ablation in mice of the mTORC components raptor, rictor, or mLST8 reveals that mTORC2 is required for signaling to Akt-FOXO and PKCalpha, but not S6K1. *Dev. Cell*, **11**, 859–871.
22. Cameron,A.J. *et al.* (2011) mTORC2 targets AGC kinases through Sin1-dependent recruitment. *Biochem. J.*, **439**, 287–297.
23. Gao,T. *et al.* (2008) The phosphatase PHLPP controls the cellular levels of protein kinase C. *J. Biol. Chem.*, **283**, 6300–6311.
24. Cameron,A.J. *et al.* (2009) PKC maturation is promoted by nucleotide pocket occupation independently of intrinsic kinase activity. *Nat. Struct. Mol. Biol.*, **16**, 624–630.
25. St Johnston,D. *et al.* (2010) Cell polarity in eggs and epithelia: parallels and diversity. *Cell*, **141**, 757–774.
26. Chen,J. *et al.* (2013) The Par3/Par6/aPKC complex and epithelial cell polarity. *Exp. Cell Res.*, **319**, 1357–1364.
27. Farquhar,M.G. *et al.* (1963) Junctional complexes in various epithelia. *J. Cell Biol.*, **17**, 375–412.
28. Nelson,W.J. (2008) Regulation of cell-cell adhesion by the cadherin-catenin complex. *Biochem. Soc. Trans.*, **36**(Pt 2), 149–155.
29. Baum,B. *et al.* (2011) Dynamics of adherens junctions in epithelial establishment, maintenance, and remodeling. *J. Cell Biol.*, **192**, 907–917.
30. Frisch,S.M. *et al.* (1994) Disruption of epithelial cell-matrix interactions induces apoptosis. *J. Cell Biol.*, **124**, 619–626.
31. Leung,C.T. *et al.* (2012) Outgrowth of single oncogene-expressing cells from suppressive epithelial environments. *Nature*, **482**, 410–413.
32. Partanen,J.I. *et al.* (2012) Tumor suppressor function of Liver kinase B1 (Lkb1) is linked to regulation of epithelial integrity. *Proc. Natl Acad. Sci. USA*, **109**, E388–E397.
33. Igaki,T. *et al.* (2006) Loss of cell polarity drives tumor growth and invasion through JNK activation in Drosophila. *Curr. Biol.*, **16**, 1139–1146.
34. Bilder,D. (2004) Epithelial polarity and proliferation control: links from the Drosophila neoplastic tumor suppressors. *Genes Dev.*, **18**, 1909–1925.
35. Thiery,J.P. (2002) Epithelial-mesenchymal transitions in tumour progression. *Nat. Rev. Cancer*, **2**, 442–454.
36. Dow,L.E. *et al.* (2007) Polarity regulators and the control of epithelial architecture, cell migration, and tumorigenesis. *Int. Rev. Cytol.*, **262**, 253–302.
37. Huang,L. *et al.* (2010) Polarity protein alterations in carcinoma: a focus on emerging roles for polarity regulators. *Curr. Opin. Genet. Dev.*, **20**, 41–50.
38. Pagliarini,R.A. *et al.* (2003) A genetic screen in Drosophila for metastatic behavior. *Science*, **302**, 1227–1231.
39. Brumby,A.M. *et al.* (2003) scribble mutants cooperate with oncogenic Ras or Notch to cause neoplastic overgrowth in Drosophila. *EMBO J.*, **22**, 5769–5779.
40. Leong,G.R. *et al.* (2009) Scribble mutants promote aPKC and JNK-dependent epithelial neoplasia independently of Crumbs. *BMC Biol.*, **7**, 62.
41. Wu,M. *et al.* (2010) Interaction between Ras(V12) and scribbled clones induces tumour growth and invasion. *Nature*, **463**, 545–548.
42. McCaffrey,L.M. *et al.* (2012) Loss of the Par3 polarity protein promotes breast tumorigenesis and metastasis. *Cancer Cell*, **22**, 601–614.
43. Iden,S. *et al.* (2012) Tumor type-dependent function of the par3 polarity protein in skin tumorigenesis. *Cancer Cell*, **22**, 389–403.
44. Akimoto,K. *et al.* (1996) EGF or PDGF receptors activate atypical PKClambda through phosphatidylinositol 3-kinase. *EMBO J.*, **15**, 788–798.
45. Baldwin,R.M. *et al.* (2008) Regulation of glioblastoma cell invasion by PKC iota and RhoB. *Oncogene*, **27**, 3587–3595.
46. Diaz-Meco,M.T. *et al.* (1994) Evidence for the *in vitro* and *in vivo* interaction of Ras with protein kinase C zeta. *J. Biol. Chem.*, **269**, 31706–31710.
47. Regala,R.P. *et al.* (2005) Atypical protein kinase Ciota plays a critical role in human lung cancer cell growth and tumorigenicity. *J. Biol. Chem.*, **280**, 31109–31115.
48. Murray,N.R. *et al.* (2004) Protein kinase Ciota is required for Ras transformation and colon carcinogenesis *in vivo*. *J. Cell Biol.*, **164**, 797–802.
49. Bjorkoy,G. *et al.* (1997) Reversion of Ras- and phosphatidylcholine-hydrolyzing phospholipase C-mediated transformation of NIH 3T3 cells by a dominant interfering mutant of protein kinase C lambda is accompanied by the loss of constitutive nuclear mitogen-activated protein kinase/extracellular signal-regulated kinase activity. *J. Biol. Chem.*, **272**, 11557–11565.
50. van Dijk,M.C. *et al.* (1997) Platelet-derived growth factor activation of mitogen-activated protein kinase depends on the sequential activation of phosphatidylcholine-specific phospholipase C, protein kinase C-zeta and Raf-1. *Biochem. J.*, **325**(Pt 2), 303–307.
51. Aranda,V. *et al.* (2006) Par6-aPKC uncouples ErbB2 induced disruption of polarized epithelial organization from proliferation control. *Nat. Cell Biol.*, **8**, 1235–1245.
52. Kobayashi,T. *et al.* (2010) Activation of Rac1 is closely related to androgen-independent cell proliferation of prostate cancer cells both *in vitro* and *in vivo*. *Mol. Endocrinol.*, **24**, 722–734.
53. Wooten,M.W. *et al.* (2001) Nerve growth factor stimulates multisite tyrosine phosphorylation and activation of the atypical protein kinase C's via a src kinase pathway. *Mol. Cell. Biol.*, **21**, 8414–8427.
54. Suzuki,A. *et al.* (2001) Atypical protein kinase C is involved in the evolutionarily conserved par protein complex and plays a critical role in establishing epithelia-specific junctional structures. *J. Cell Biol.*, **152**, 1183–1196.
55. Georgiou,M. *et al.* (2008) Cdc42, Par6, and aPKC regulate Arp2/3-mediated endocytosis to control local adherens junction stability. *Curr. Biol.*, **18**, 1631–1638.
56. Suzuki,A. *et al.* (2004) aPKC acts upstream of PAR-1b in both the establishment and maintenance of mammalian epithelial polarity. *Curr. Biol.*, **14**, 1425–1435.
57. Debnath,J. *et al.* (2005) Modelling glandular epithelial cancers in three-dimensional cultures. *Nat. Rev. Cancer*, **5**, 675–688.
58. Lubarsky,B. *et al.* (2003) Tube morphogenesis: making and shaping biological tubes. *Cell*, **112**, 19–28.
59. O'Brien,L.E. *et al.* (2001) Rac1 orientates epithelial apical polarity through effects on basolateral laminin assembly. *Nat. Cell Biol.*, **3**, 831–838.
60. Durgan,J. *et al.* (2011) Par6B and atypical PKC regulate mitotic spindle orientation during epithelial morphogenesis. *J. Biol. Chem.*, **286**, 12461–12474.
61. Horikoshi,Y. *et al.* (2009) Interaction between PAR-3 and the aPKC-PAR-6 complex is indispensable for apical domain development of epithelial cells. *J. Cell Sci.*, **122**(Pt 10), 1595–1606.

62. Hao,Y. *et al.* (2010) Par3 controls epithelial spindle orientation by aPKC-mediated phosphorylation of apical Pins. *Curr. Biol*., **20**, 1809–1818.
63. Khwaja,A. *et al.* (1997) Matrix adhesion and Ras transformation both activate a phosphoinositide 3-OH kinase and protein kinase B/Akt cellular survival pathway. *EMBO J*., **16**, 2783–2793.
64. Lee,G.Y. *et al.* (2007) Three-dimensional culture models of normal and malignant breast epithelial cells. *Nat. Methods*, **4**, 359–365.
65. Bentires-Alj,M. *et al.* (2006) A role for the scaffolding adapter GAB2 in breast cancer. *Nat. Med*., **12**, 114–121.
66. Reynolds,A.B. *et al.* (1987) Activation of the oncogenic potential of the avian cellular src protein by specific structural alteration of the carboxy terminus. *EMBO J*., **6**, 2359–2364.
67. Gould,C.M. *et al.* (2008) The life and death of protein kinase C. *Curr. Drug Targets*, **9**, 614–625.
68. Kim,M. *et al.* (2007) Polarity proteins PAR6 and aPKC regulate cell death through GSK-3beta in 3D epithelial morphogenesis. *J. Cell Sci*., **120**(Pt 14), 2309–2317.
69. Kjaer,S. *et al.* (2013) Adenosine-binding motif mimicry and cellular effects of a thieno[2,3-d]pyrimidine-based chemical inhibitor of atypical protein kinase C isozymes. *Biochem. J.*, **451**, 329–342.
70. Gschwendt,M. *et al.* (1996) Inhibition of protein kinase C mu by various inhibitors. Differentiation from protein kinase c isoenzymes. *FEBS Lett*., **392**, 77–80.
71. Lai,K.C. *et al.* (2013) Depleting IFIT2 mediates atypical PKC signaling to enhance the migration and metastatic activity of oral squamous cell carcinoma cells. *Oncogene*, **32**, 3686–3697.
72. Cameron,A.J. *et al.* (2007) Protein kinases, from B to C. *Biochem. Soc. Trans*., **35**(Pt 5), 1013–1017.
73. Standaert,M.L. *et al.* (2001) Insulin and PIP3 activate PKC-zeta by mechanisms that are both dependent and independent of phosphorylation of activation loop (T410) and autophosphorylation (T560) sites. *Biochemistry*, **40**, 249–255.
74. Liu,H. *et al.* (2004) Polarity and proliferation are controlled by distinct signaling pathways downstream of PI3-kinase in breast epithelial tumor cells. *J. Cell Biol*., **164**, 603–612.
75. Palmer,R.H. *et al.* (1995) Activation of PRK1 by phosphatidylinositol 4,5-bisphosphate and phosphatidylinositol 3,4,5-trisphosphate. A comparison with protein kinase C isotypes. *J. Biol. Chem*., **270**, 22412–22416.
76. Qiu,R.G. *et al.* (1995) An essential role for Rac in Ras transformation. *Nature*, **374**, 457–459.
77. Zhang,L. *et al.* (2006) Integrative genomic analysis of protein kinase C (PKC) family identifies PKCiota as a biomarker and potential oncogene in ovarian carcinoma. *Cancer Res*., **66**, 4627–4635.
78. Regala,R.P. *et al.* (2009) Atypical protein kinase C{iota} is required for bronchioalveolar stem cell expansion and lung tumorigenesis. *Cancer Res*., **69**, 7603–7611.

Received April 1, 2013; revised August 7, 2013; accepted August 24, 2013